The failure analysis of the drilling rig hoisting steel wire rope

Pavel Peterka [a]*, Jozef Krešák [a], Marek Vojtko [b], Branislav Halek [c], David Heinz [c]

[a]Faculty of Mining, Ecology, Process Control and Geotechnology, Technical University of Kosice, Park Komenskeho 14, 042 00 Kosice, Slovak Republic
[b]Institute of Materials Research, Slovak Academy of Science, Watsonova 47, 040 01 Košice, Slovak Republic
[c]Faculty of Mining, Ecology, Process Control and Geotechnology, Technical University of Kosice, Park Komenskeho 14, 042 00 Kosice, Slovak Republic

Highlights

- Use of ropes in systems with lower safety level.
- Added energy absorbed by non-slipped rope length indicates degree of rope fatigue.
- Failure in following of rules stated for rope pulling causes rapid rope fatigue.
- Monitoring of rope condition by NDT and by evaluation of ton-kilometres.

Abstract

Drilling rigs belong to the lowest-safety level of hoisting rope systems. The valid regulation for drilling permits the usage of steel ropes on condition that their permanent safety does not decrease under the value 2.5. Considerable dynamic and cyclic stresses, abrasion and corrosive environment generated during the operation cause rapid fatigue and rope damage. The stress of the rope in operation leads to the specific precautions ensuring the safety rope work. The specific precautions include monitoring of the rope tractive work measured in tonne-kilometres (ton-kilometres services). The working part of the hoisting ropes of the drilling rigs - after the stated number of tonne kilometres was worked off - is slipped and a regular non-destructive rope test (NDT) is recommended. Rope under sizing, failing in rope slipping program and non- implementation of NDT controls led to the situations endangering the drilling crew safety. After the critical situations the operator decided to perform the analysis of the condition of all ropes.

Keywords

wire rope, fatigue failure, cracks, NDT.

1. Intrduction

Considerable dynamic and cyclic stresses, abrasion, adhesion and corrosive environment generated during the operation cause rapid fatigue and rope damage. The stress of the rope in the operation leads to the specific precautions ensuring the safety rope work. The length of the rope service depends on the quality of the rope wires material, the rope construction and of the rope service conditions. The metallurgical quality of the wire material has a direct influence on the rope service life length; this well-known axiom is supported by works of many authors [36, 22, 8]. Specific conditions of a rope operation make rope manufacturers to develop new and special construction of ropes. This structural diversity of ropes requires more specific skills of rope users [18]. The choice of the rope quality and rope construction depends on an operator; this process is affected by finances and service conditions mostly.

The work conditions are the most specific and they depend on a place of operation (mines, elevators, cableways, hoisting system, drilling rigs). The rope employment length plus the continues degeneration of ropes lead to a fatigue failure of the rope wires [27]. The works of Chang et al. deal with wear mechanism of ropes under a working stress in mining industry [3, 6]. Fatigue and adhesion wear Chang et al. consider to be the major wear mechanisms [4]. The wear of ropes could be caused by combination of the inside and the outside mechanisms. The outside wear background stems in any interaction between rope way parts like rope pulley, hoist drum and the rope in multilayer winding hoist.

Peng et al. specified another two outside wear mechanisms of ropes - friction and impact [23]. Inside wear of a rope is caused by any interaction between rope wires and rope strands mostly. The fundamental mechanism of the inside wear is any dynamic contact between rope wires or rope strands [29].The combination of the wear mechanisms leads to the decrease of the breaking force of the rope [5]. The choice of the proper rope construction for the specific rope employment, knowledge of specific rope service conditions and wear mechanisms are fundamental for safety rope operation.

It is important to pay attention to two another factors affecting safety rope operations, rope maintenance and rope pulling system, the rope condition monitoring.

Lubrication protects ropes against corrosion and wear of the outer rope wires during interaction between ropes and rope pulley system parts; lubrication protects inner wires during any interaction between wires inside rope construction as well. Pal et al. deal with the influence of inadequate lubrication on wear of internal rope wires [21]. The interaction between a rope and a pulley causes any wear of them [17]. Correct friction forces and wrap angle between a rope and pulley is fundamental for rope operation. Kou et al. presented dependence between the rope transverse vibration and the real contact area of the

(*) Corresponding author.
E-mail addresses: P. Peterka - pavel.peterka@tuke.sk, J. Krešák - jozef.kresak@tuke.sk, M. Vojtko - mvojtko@saske.sk, B. Halek - branislav.halek@tuke.sk, D. Heinz - david.heinz@tuke.sk

rope [11]. Guo et al. describe dependence between the rope longitudinal vibration and the friction forces [9]. The corrosion process of ropes is the most significant in the most areas of ropes employment. The petroleum industry is specified by using various chemical agents. The works of Marandi et al., Wang et al, and Li et al. deal with the influence of chemical agent on wire ropes [13, 19, 30].

The non-destruction testing brings review of real rope conditions in operation [15, 32, 33]. The detection of the broken wires and loss of metallic cross section by the NDT device enables to perform risk analyses pursuant to safety standards [7, 12, 34]. Dynamic and cyclic work of drilling rig hoist system and a low limit of rope safety bring a specific form of rope operation. The rope fatigue is monitored by the ton-kilometres service value in the process of operation. The safety of the rope operation is assured by the rope slipping process. Many authors investigated fatigue life of ropes. Piskoty et al. studied processes of the sharp bending of the ropes [26]. Wang et al. presented the mechanisms of the crack propagations under the large fatigue cycles [31].Zhao et al.investigated influence of the low/high fatigue cycles on the rope wires and presented the fatigue life prediction method for the ropes [37]. The fatigue process of the ropes was investigated by Lorenco et al. too [16]. Vukelic and Vizentin focused on dependence of the rope cross section area size and remaining service life of the ropes [28]. Liang et al. analysed dynamic rope response on the number of wire breaks [14]. Celik and Guloksuz presented a new distribution of the rope lifetime. They defined the function of the reliability, mean time to failure and hazard function for this distribution [2]. Zhang et al. focus on the reliability analysis for the multiple-phased mission system [35].Młynarski et al. presented the models of the preventive maintenance strategy. They focused on the determination of the joint time of preventive maintenance [20]. The corrective maintenance model was estimated by Andrzejczak et al. [1]. Multi-state operation systems were studied by Knopik and Migawa. They created the age replacement model for technical objects [10].

In our paper the fatigue life and operation of drilling rig hoist system are monitored by the different system to the systems mentioned above. In our case the rope slipping process does not allow to use standard ways for fatigue life monitoring and remaining service life prediction. The drilling rig pulley system operator needs the complex of information: the rope parameters, the ton kilometers service monitoring values, the real rope condition earned by the NDT and the maintenance service information. The information analysis can reveal the correct process of the slipping process calculation and the evaluation of the remaining service life of the rope. Neglecting or omitting one of these points leads to the reduction of the service life of the rope and also to critical situations.

2. Theory and calculation

According to the current regulations issued for organizations performing their activities under the supervision of the Slovak Mining Authority (SBU) the hoist rope can be safely used until the permanent safety of the rope falls below 2.5 due to its depreciation consideringthe highest static load of the drilling rig (SBU Decrees No. 8/1981 and No. 88/1986 §16 paragraph 1).

In the oil and gas industry the safety degree and the method of slipping a rope is stated according to the API Recommended Practice 9B. This standard sets a safety rating of 3.0 for rotary drilling hoist systems. This level is even higher than the above specified legal boundary.

The structure of the rope; the minimum breaking load of the rope (F_{min} [kN]); the number of strings of the hoisting rope (N) and the efficiency of the machine-tool system (η_m) have the influence on the estimation of the safety level of the rope (f). The pulley system of the analysed drilling rig allows reeling of the rope with winding 5x6 (Fig. 1) or 4x5 (Fig. 2). In the case of the 5x6 winding the pulley system has 10 strings. In the case of the 4x5 winding the pulley system has 8 strings.

The safety degree (f) can be determined according to the API Recommended Practice 9B as follows:

$$f = F_{min} / F_B; [-]\tag{1}$$

where:
$$F_B = F_H / (N\eta_m); [kN]\tag{2}$$

where :
$$\eta_m = (K^N - 1) / (N.(K-1).K^N); [-]\tag{3}$$

where: K – friction index of the pulley bearings [-];
    for pulley sliding bearing stands K = 1,09;
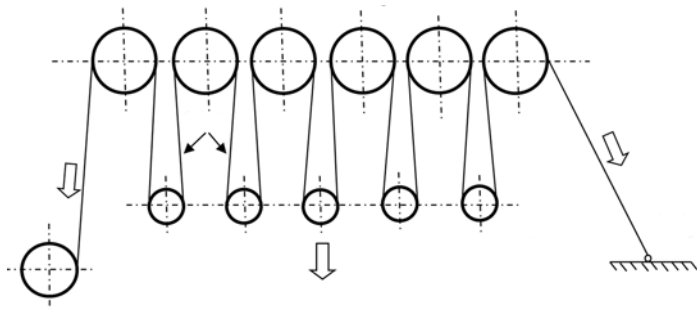   for pulley rolling bearing stands K = 1,04;

Fig. 1. *The pulley system of the drilling rig, winding of the hoisting rope 5x6 - ten strings. Where: F_H - hook load [kN]; F_B – tensile force in a branch threading up on the drum [kN]; F_D - tensile force in the dead end of the rope[kN]*
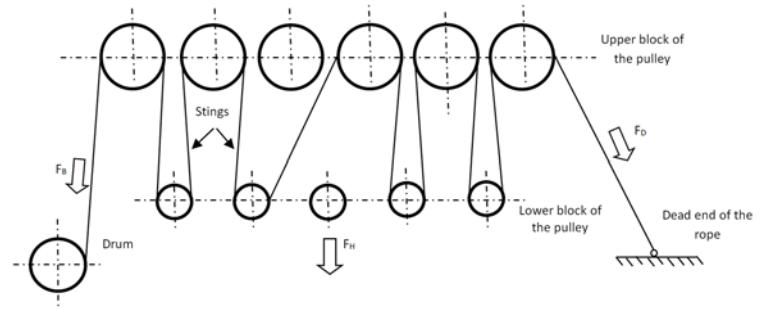

Fig. 2. *The pulley system of the drilling rig, winding of the hoisting rope 4x5- eight strings*

The Standard API RP9B according to the height of the drilling tower and the diameter of the drum of the drilling rig hoist system determines the slipped length of the rope. Based on the diameter of the put on rope, the height of the drilling tower and the difficultness of the drilling process the Standard API RP9B specifies the interval
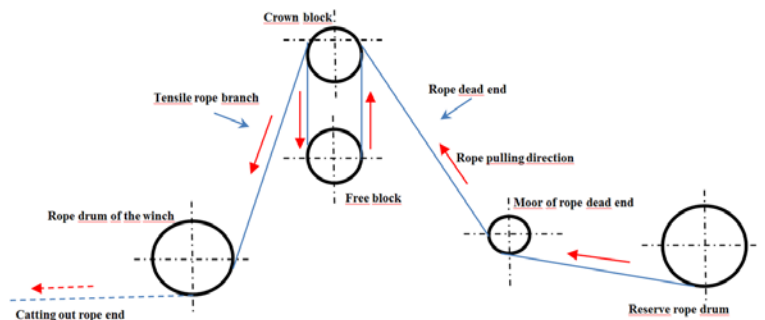

Fig. 3. *The drilling rig hoist system – rope pulling system strings*

of total rope work in tonne-kilometres (ton-kilometers service); the rope has to be slipped when it is reached. The standard API RP9B sets the prescribed interval of ton-kilometers service for the safety value 5. Subsequently, we adjust the set value using the corrective coefficient (z) which is given by the equation:

Fig. 4. The course of the NDT record (both directions of the rope motion; differential coil)

$$z = -0,0147f^2 + 0,3259f - 0,264 \, [-] \qquad (4)$$

3. Material and methods

The rope operating in the hoist system for 53 days was subjected to the analysis. The rope was not monitored by the NDT methods during the operation, its ton-kilometers service was monitored and the rope was regularly slipped. The damage of the rope caused by numerous fractures was detected, therefore the operator decided to perform the analysis of damages. The rope was subjected to the following tests: the NDT examination to measure the amount of the damage, mechanical tests to identify mechanical properties of the rope, metallographic and fractographic tests of the material of the rope wires. The analysis of the load of the rope in operation by determining the ton-kilometers service of the rope was added on.

The rope constructed according to the EN 12385-2: 28,0 6x27NS SFC 1570 U sZ was put on into the drilling rig pulley system.

Table 1. Parameters of the monitored rope

the rope manufactured according to	EN 12385-4+A1:2008-07
the construction of the rope	6x(1+6+10+10) + v(SFC)
the number of wires in the rope	162
the diameter of the rope	28 mm
the rope wire surface finish	uncoated
the rope grade	1570 MPa
the minimum aggregate breaking force	500.8 kN
the minimum breaking force	430.7 kN
The rope core material	SFC - polypropylene
the nominal metallic cross-section of the rope	318.9 mm^2
the rope nominal mass	2.93 kg.m^{-1}

Table 2. The dimensions of the rope wires under examination.

Rope core / strand	Number of the strands	Number of the wires	Wire diameter [mm]
Strands	6	1	1.10
		6	1.00
		10	1.28
		10	2.10
Core	3	Polypropylene ϕ 14mm	

Table 3. Methods used to assess the mechanical properties of the rope wires.

applied methods of rope assessment	ways of testing	criteria of testing and preparation of sample	assessment criteria
mechanical testing of wires of the new rope	diameter of the wire	EN 10218-2	EN 12385-1 Anex B EN 10264-2
	strength	EN ISO 6892-1	
	reverse bend	ISO 7801	
	torsion	ISO 7800	
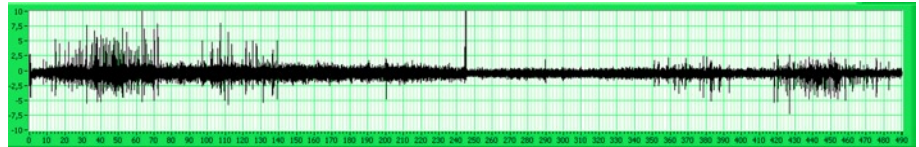
Methods used to assess the mechanical properties of the rope wires (Table 3).

4. Results

4.1. Non-destructive rope examination

The hoisting rope of the drill rig was subjected to the NDT control at the maximum possible length, i.e. 245m in both directions of the rope motion (Fig. 4). The measured rope diameter was in the interval 28.2mm - 28.1 mm.

The NDT control revealed the increased number of local fractures in the working part of the rope (Fig. 5). All the fractures of the wires were located on the surface of the rope strands.
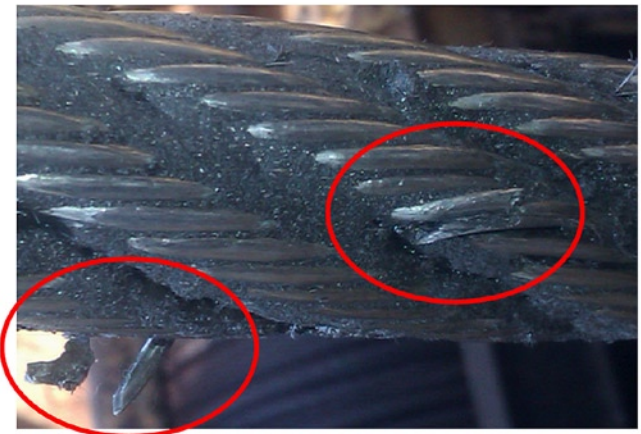

Fig. 5. The detail of the place with two local ruptures of the rope wires

The diminution of the metal cross-section was evaluated for the largest wire diameter in the rope 2.10 mm (3.46 mm^2) forming the upper contact layer of the strand; it represents a loss 1.085% (3.46mm^2 / 318.9mm^2) of the metal cross - section. The wire with the diameter 2.10 mm shows the diminution 1.085% (3.46mm^2 / 318.9mm^2) of the metal cross-section:

$$X = s_d / s_l; \, [\%] \qquad (5)$$

where: X- diminution of the rope metal cross- section [%],
S_d – cross – section of the wire [mm^2],
S_l - metal cross-section of the rope [mm^2].

At the point where three local fractures occurred the loss of the metal cross-section was 3.25% (3x1.085%, i.e. yardage 14.7m; 32.2m; 37.1m; 38.2m; 40.2m; 55.7m). At the point where four local fractures appeared the diminution was 4.34% (4x1.085%, i.e. 39.2m; 50.4m 51.5m). The yardage 47.5m shoved five ruptures, the loss of metal cross-section was 5.42% (5x1.085%).

4.2. Mechanical tests

The sample taken from the undamaged part of the hoisting rope was subjected to the following mechanical tests: tear strength test (Fig. 6), reverse bend-
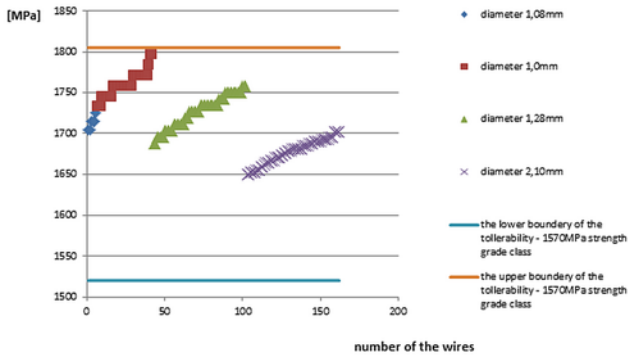
Fig. 6. The strengths grade courses for individual wires

Vertical lines and values (Fig. 7) - the tolerance criteria for torsion in accordance with the EN 10264-2 with their modification according to the EN 12385-1 Annex B.

The results of the above mentioned mechanical tests showed that the rope was manufactured in accordance with the valid standard and its mechanical properties are satisfactory.

4.3. Metallographic and fractographic tests

The material of the wires has a characteristic ferritic-pearlitic microstructure with a strong line arrangement of ferrite and pearlite (Fig. 8). This line spacing is a result of the intensive plastic deformation caused by pulling of wires in cold weather condition. The monitoring of the wire surface in both longitudinal and transverse directions has shown that the microstructure does not show signs of decarburization
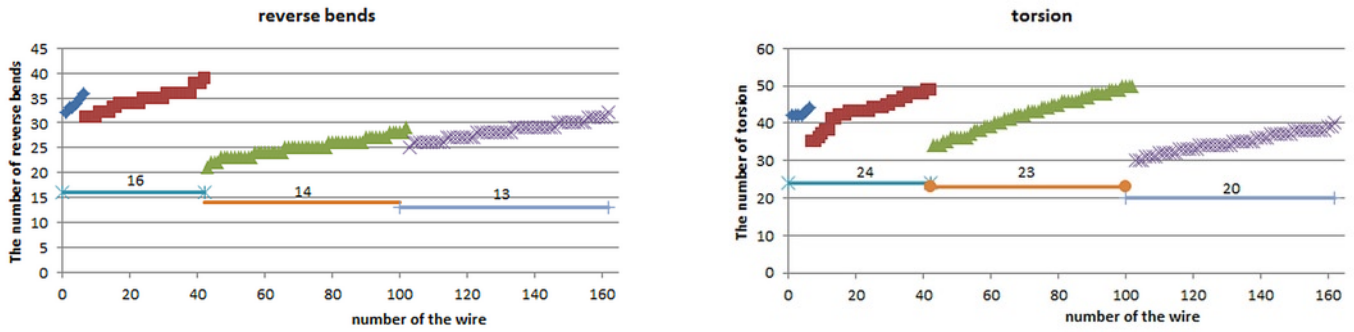

Fig. 7. The course of the results: a) the reverse bending test of the wires. Vertical line and value - the tolerance criteria for reverse bending according to the EN 12385-1 Annex B; b) the course of the torsion test results
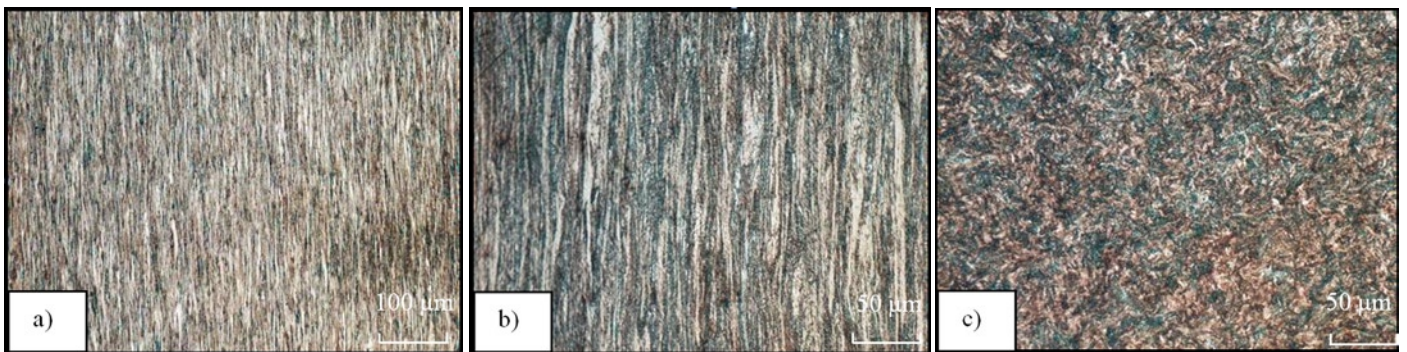

Fig. 8 Line spacing of ferritic-pearlitic microstructure. (a) 100x in the longitudinal direction; b) 500x in the longitudinal direction; c) 500x in the transversal direction.
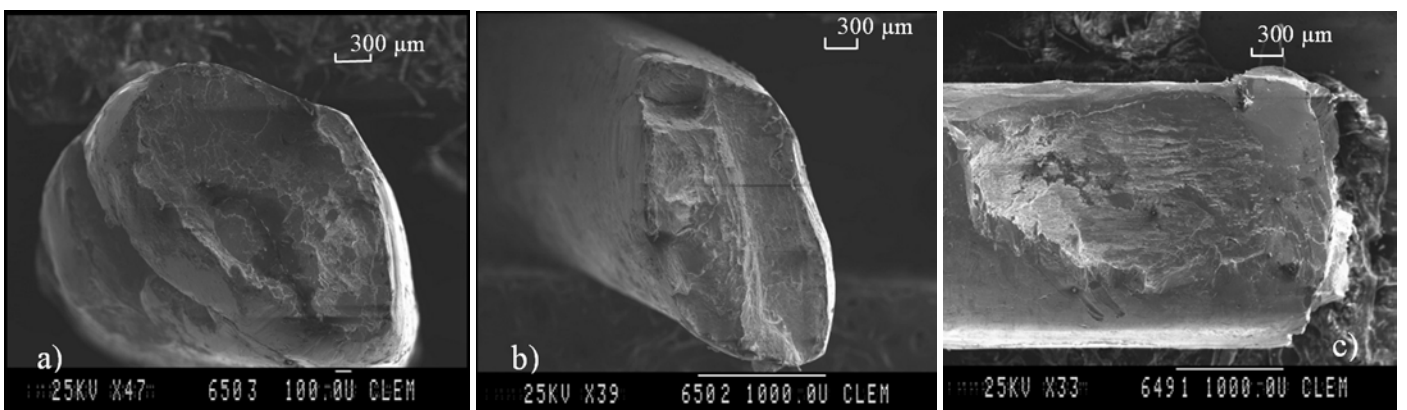

Fig. 9. The wire deformation. a); b) in the area of the fracture; c) the side view

ing test and torsion test (Fig. 7) according to the standards listed in the Table 3.

The tolerance criterion for a rope wire strength according to the EN 12385-1 Annex B is set at: 1520MPa (-50MPa; lower boundary) and 1805MPa (+ 15%; upper boundary) (Fig. 6).

in these areas (Fig. 8 a, b, c).

Fractographic analysis performed by the scanning electron microscope reveals that the wires show features of an intensive plastic deformation before a failure. The cross-section of the wires (originally
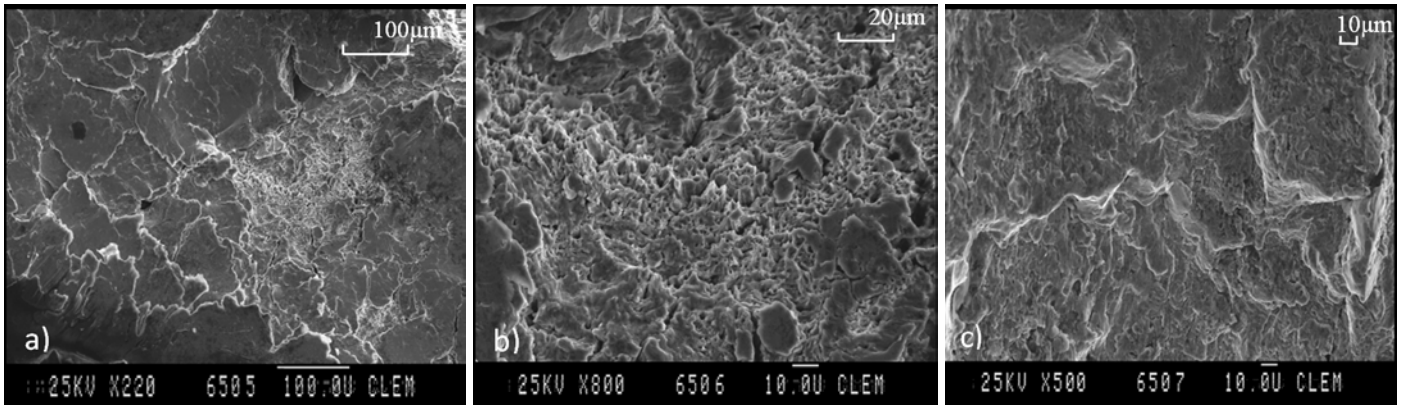
Fig. 10. *The wire sample under the scanning electron microscope. (a) transcrystalline ductile failure – on the right in the center; (b) the detail of the transcrystalline ductile failure (a); (c) the imprinted fracture area of the wire*
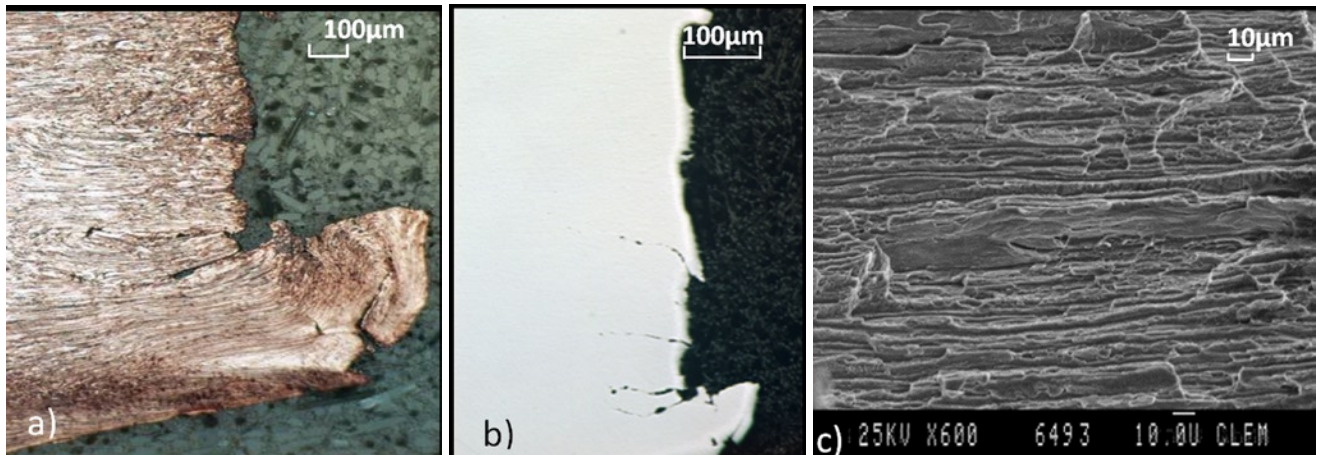

Fig. 11. *The wire deformation (a) the intensive plastic deformation of the material around the fracture; b) metallographic cuts of wires c) the secondary material cracks*

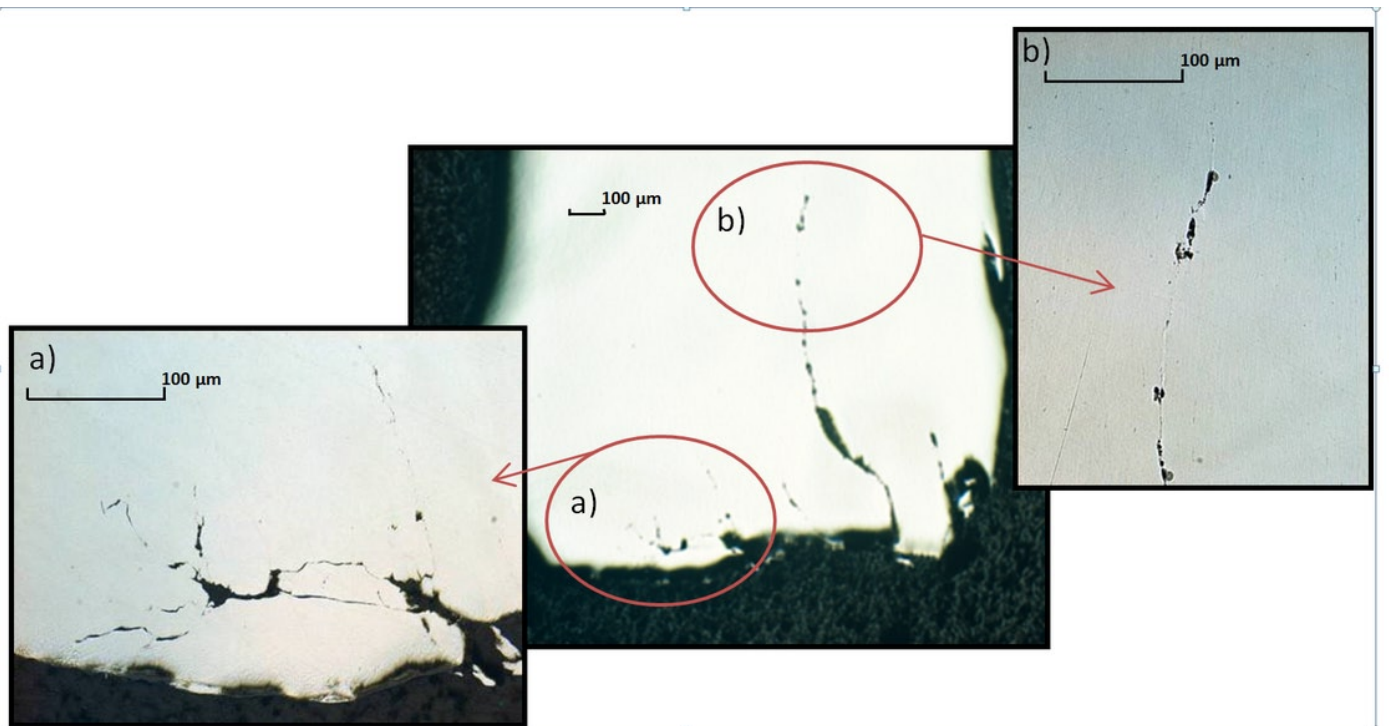Fig. 12. *Metallographic cut of the wire; a) detail of the cracks; b) detail of the cracks.*

circular) is significantly deformed not only around the fracture surface but also in the adjacent areas (Fig. 9).

The analysis of the wire deformations confirmed the intensive plastic deformation of the material around the rupture of the wires with secondary cracks propagating perpendicularly to the anaclastic sur-

face in the direction of the wire axis and following the raster scan of ferrite and perlite (Fig. 12b).

The number, size, pattern of the inclusions on non-etched metallographic patterns in longitudinal (wire axis direction) direction and transverse direction were evaluated. The following pictures illustrate the appearance, length and orientation of the cracks around the fracture surface. The material does not show excessive pollution. The amount, size and shape of the inclusions is normal for this steel type. As it is shown in Fig. 12 the cracks in the neighborhood of the fracture surface are approximately oriented in the direction of the wire axis. The net and branching of cracks occur in the areas with severe plastic deformation.

4.4. The hoisting rope safety analysis

Pursuant to the parameters of the monitored rope and the drilling rig pulley system the safety of the monitored rope was determined. The use of the equations (1) to (3) leads to the following findings:
- the rope winding in the 4x5 pulley system with 8 strings, maximum load capacity 145t, roller bearings with friction coefficient K = 1.04 and minimum rope load capacity 430.7 kN: the rope safety is 2.04;
- the rope windings in the 5x6 pulley system with 10 strings, maximum load capacity 145t, roller bearings with a friction co-

efficient K = 1.04 and minimum rope load capacity 430.7 kN: the rope safety is 2.46.

The pulley winding had 10 strings (information provided by the operator) - the security value 2.46 is lower than the legally permitted security value 2.5. This shows that any further reduction of the wire rope metal cross-section caused by the disruption of the wire leads to the decrease of the safety of the rope. The NDT inspection revealed a high number of wire ruptures creating the nests in many places, thereby reducing the metal cross-section and the rope load capacity. Considering the value of the minimum rope tonnage allows to speculate on the following decreases of the safety parameters of the rope. The parameters are listed in the Table 4 and the subsequent calculations are accomplished according to the equations (1) to (3). Whereby in the equation (1) a reduced minimum rope load due to the diminution of the rope metal cross-section was considered. The minimum load was calculated according to the equation (6):

$$F_{min} = F'_{min}\big((100 - X)/100\big);[kN] \qquad (6)$$

where: F_{min} - the reduced minimum breaking force due to the reduction of the metal cross-section of the rope [kN];

F'_{min} - minimum breaking force stated by the manufacturer [kN]; (430.7kN);

Table 4. Overview of the approximate decline in rope safety at locations with increased amount local fractures

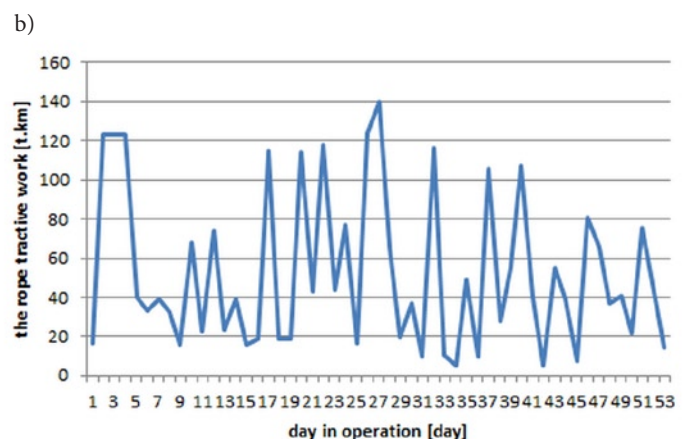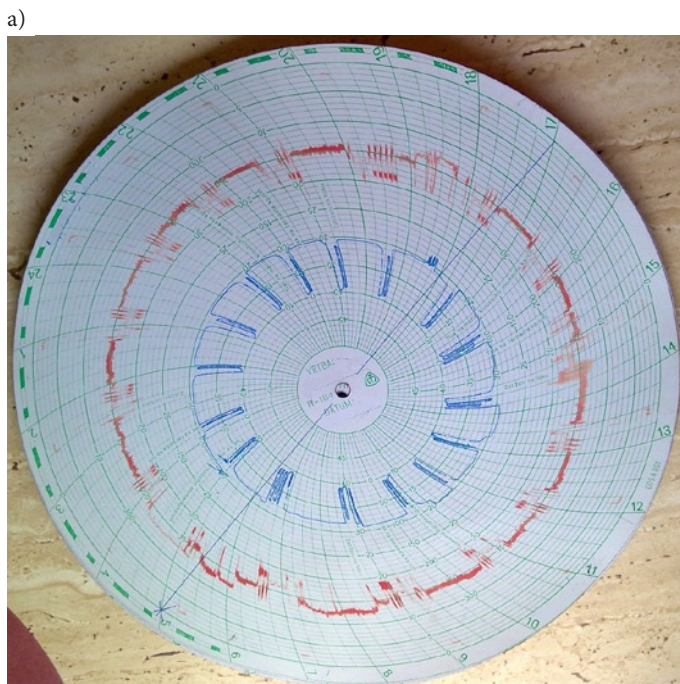| Number of rope strings [N]	Efficiency	m_H [kg]	K	F_H [kN]	number of disruptions		
					3	4	5
					the loss of metal cross-section		
					3,25 %	4,34 %	5,42 %
					F_{min}		
					416,7	412,0	407,35
					Safety of the rope „f"		
8	0.84	145	1.04	1422.45	1,97	1,95	1,93
10	0.81	145	1.04	1422.45	2,38	2,35	2,32

a)

b)

Fig. 13. The rope tractive work (ton-kilometers) a) source for evaluating the total daily rope work of the rope; b) processed course of the total rope tractive works per day during the monitored period

Table 5. The summary of the rope slipping, actual rope slipping program

A* [tkm]	262	163	347	168	430	348	227	144	162	332	195
slipping [m]	10.69	6.65	14.16	6.88	17.54	14.22	9.27	5.87	6.6	13.53	NDT

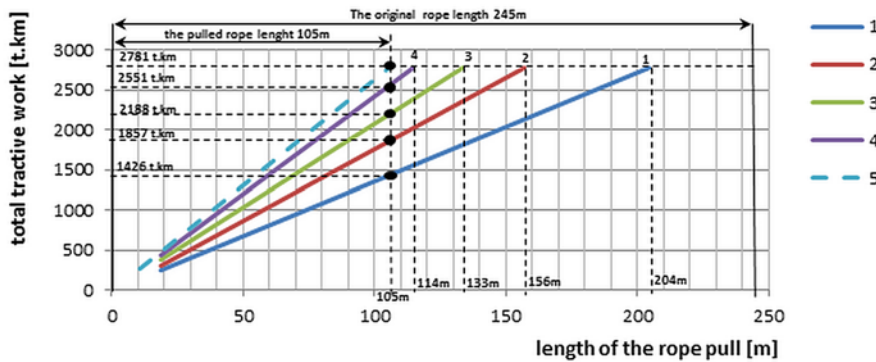*The interval of the tractive work (ton-kilometers) for slipping [tkm].

Fig. 14. The runs of the slipping of the rope in dependence on the sum of the overall tractive work (ton-kilometers) of the rope (according API RP9B). The model courses: 1- slipping interval 247tkm; 2 - slipping interval 313tkm; 3– slipping interval 378tkm; 4 – slipping interval 444tkm; 5 (dashed) – monitored actual slipping of the rope (451tkm)
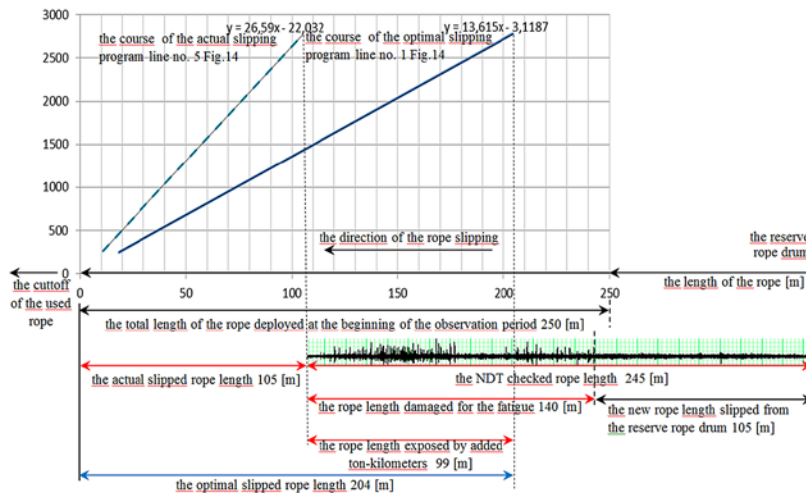

Fig. 15. The analysis of the fatigue rope damage, X - diminution of the metal rope cross-section [%]

The way how to evaluate rope fatigue rates is to determine the amount of added energy (ton-kilometers) absorbed by non-slipped length of the rope. The daily load record of the drilling rig obtained from the tonometer (Fig.13a) is used as a data source for the total tractive work (ton-kilometers) evaluation of the rope per day.

The evaluation of the tractive work (ton-kilometers) of the monitored rope was carried out from the moment the rope was put on into the hoist to the NDT control led to the decision to slipping the rope along the whole working length (Fig. 4).The observed operating period of the rope was 53 days. The total daily work (ton-kilometers) of the rope according to [24] [25] (Fig. 13b) was evaluated on the base of the daily hook load records during this period. The operator defined the value of the total tractive work (ton-kilometers) for the given drilling rig up to the first rope slipping for the value 451 t.km - the length of the slipped section of the rope was 18.4m (Fig.14, dashed line 5). During the operation of the drilling rig the rope was slipped in the following intervals listed in the Table 5.

During the monitored time interval the rope was slipped globally cca. 105 m (total sum of slipping Table 5).

Referring to the regulations of the Standard API RP 9B the intervals of slipping can be divided into four variants according to the volume of work done by the drilling rig and also safety. The course of the individual model variants in terms of the Standard API RP9B and the actual courses of slipping shows the Fig. 14.

5. Discussion

The detailed analysis of the places damage by ruptures was due to the repeated intensive plastic deformation caused by the low cycle fatigue process. The wire material was subjected to a multiple load stress greater than the yield point at which the original wire cross-section was deformed. A normal force fracture occurred when the plasticity reserve was run out; - obviously, the rope was wrongly slipped while it was working.

The above mentioned analyses showed the incorrectly chosen construction of the rope and also incorrectly determined the system safety (the value of safety directly determines the interval of the rope ton-kilometers performed during one slipping). The 451 t.km / 18.4 m slipping interval chosen by the operator was set according the incorrect safety analysis. As the initial rope tonnage the minimum aggregate breaking force (500.8 kN) was used instead of the minimum breaking force (430.7 kN). The security defined upon the minimum aggregate breaking force is 2.85. The correct value is 2.46 pursuant to the minimum breaking force.

By analysing the individual model variants of slipping according to the API RP9B methodology (Fig. 14) and comparing them with the actual slipping process the following conclusions regarding the reasons for rope fatigue were reached (Fig. 15).

The NDT check was performed on the monitored rope at the sum of the total tractive work (ton-kilometers) of 2871 t.km. The rope was slipped up to 105m total. Upon the results of the NDT it was decided to slipping else 140m of the rope. After the projection of these facts into the courses shown in the Fig. 15 it is clear that the procedure of the rope slipping is incorrect.

Apart from the facts (improper rope construction, improper interval of slipping, the model variants of the slippingaccording the API RP9B, Fig. 13 the model line 1 (Fig. 14, line 1, the rope slipping interval 247t.km/18.4m) is considered to be the most suitable course of the rope slipping program (Fig. 15). The model line 1 (Fig. 14 and Fig. 15) shows that the rope had to be slipped for 204m totally. This could enable all the fatigue damaged parts of the rope to circulate out of the hoist system during the drilling process. Thus, the slipping model line 1 (Fig.15) could provide an adequate redistribution of the absorbed energy into a longer rope length. The comparison of the actual, observed course (dashed line 5 Fig.15) and the model line 1 (Fig.15) shows following: when the rope was slipped for 105m the

non-slipped rest of the rope absorbed more energy than it had to absorb in the proper slipping process (Fig.15).

6. Conclusion

The hoisting rope analysis revealed the non-observance of the standard rules stated for the work of hoisting ropes of drilling rigs. The put on hoisting rope had lower safety than the standard safety required by the law when it was employed.

The rope was probably wrongly slipped while it was working (Fig. 15). These facts caused the fatigue of the rope and the formation of numerous local ruptures on the rope detected by the NDT inspection.

According to the results of the above mentioned analyses the operator is recommended :

– in the case of extremely heavily loaded ropes to carry out the NDT of the rope in addition to the measurement of tractive work (ton-kilometers) of a rope ;

– to increase the safety of the working ropes by using ropes with the IWRC core;

– to assign the intervals of slipping of the ropes in the pulley system and to lengthen the slipped segment of the rope depending on the quality of the rope.

The whole analysis confirms the necessity of the NDT performance as a control of the correctly selected slipping intervals and control of the real condition of the rope.

References

1. Andrzejczak K, Młyńczak M, Selech J. Poisson-distributed failures in the predicting of the cost of corrective maintenance. Eksploatacja i Niezawodnosc - Maintenance and Reliability 2018; 20 (4): 602-609, https://doi.org/10.17531/ein.2018.4.11.
2. Celik N, Guloksuz CT. A new lifetime distribution. Eksploatacja i Niezawodnosc - Maintenance and Reliability 2017; 19 (4): 634-639, https://doi.org/10.17531/ein.2017.4.18.
3. Chang X D, Peng Y X, Zhu Z C, Zou S Y, Gong X S, Xu C M. Evolution Properties of Tribological Parameters for Steel Wire Rope under Sliding Contact Conditions. Metals (Basel) 2018; 8: 743, https://doi.org/10.3390/met8100743.
4. Chang X, Peng Y, Zhu Z, Gong X. Breaking failure analysis and finite element simulation of wear-out winding hoist wire rope. Engineering Failure Analysis 2018; 95: 1-17, https://doi.org/10.1016/j.engfailanal.2018.08.027.
5. Chang X D, Peng Y X, Zhu Z C. Experimental investigation of mechanical response and fracture failure behavior of wire rope with different given surface wear. Tribology International 2018; 119: 208-221, https://doi.org/10.1016/j.triboint.2017.11.004.
6. Chang X D, Peng Y X, Zhu Z C, Zou S Y, Gong X S, XU C M. Effect of wear scar characteristics on the bearing capacity and fracture failure behavior of winding hoist wire rope. Tribology International 2019; 130: 270-283, https://doi.org/10.1016/j.triboint.2018.09.023.
7. Čereška A, Zavadskas E K, Bucinskas V, Podvezko V, Sutinys E. Analysis of Steel Wire Rope Diagnostic Data Applying Multi-Criteria Methods. Applied Sciences, 2018; 8: 260, https://doi.org/10.3390/app8020260.
8. Grygier D. The impact of operation of elastomeric track chains on the selected properties of the steel cord wires. Eksploatacja i Niezawodnosc - Maintenance and Reliability 2017; 19: 95-101, https://doi.org/10.17531/ein.2017.1.13.
9. Guo Y, Zhang D, Chen K, Feng C, Ge S. Longitudinal dynamic characteristics of steel wire rope in a friction hoisting system and its coupling effect with friction transmission. Tribology International 2018; 119: 731-743, https://doi.org/10.1016/j.triboint.2017.12.014.
10. Knopik L, Migawa K. Multi-state model of maintenance policy. Eksploatacja i Niezawodnosc - Maintenance and Reliability 2018; 20 (1): 125-130, https://doi.org/10.17531/ein.2018.1.16.
11. Kou B, Liu Q, Li N. Research on transverse vibration characteristics of rope change device with clamping chain transmission in lifting system. Journal of Vibroengineering 2017 19: 894-907, https://doi.org/10.21595/jve.2017.18188.
12. Kuľka J, Mantič M, Kopas M, Faltinova E. Locking the Movement of Persons on the Bridge Crane. Advances in Science and Technology Research Journal 2018; 12: 260-265, https://doi.org/10.12913/22998624/92459.
13. Li C Y, Wang J H, Zhi Y R, Wang Z R, Gong J H, Jiang J C. A dynamic prediction method for probability of rupture accidents of a chloride process based on experimental corrosion data. Journal of Loss Prevention in the Process Industries 2018; 56: 467-477, https://doi.org/10.1016/j.jlp.2018.10.007.
14. Liang B, Zhao Z, Wu X, Liu H. The establishment of a numerical model for structural cables including friction. Journal of Constructional Steel Research 2017 139: 424-436, https://doi.org/10.1016/j.jcsr.2017.09.031.
15. Liu X, Xiao J, Wu B, He C. A novel sensor to measure the biased pulse magnetic response in steel stay cable for the detection of surface and internal flaws. Sensors and Actuators A: Physical 2018; 269: 218-226, https://doi.org/10.1016/j.sna.2017.11.005.
16. Lourenco J M, Pereira F G L, Bernardini P A N, de Carvalho L A. Análise De Falha Em Um Cabo De Aço Usado Em Máquinas Apolete. Holos 2018; 4: 75-88, https://doi.org/10.15628/holos.2018.7380.
17. Ma W, Lubrecht A A. Detailed contact pressure between wire rope and friction lining. Tribology International 2017; 109: 238-245, https://doi.org/10.1016/j.triboint.2016.12.051.
18. Mańka E, Słomion M, Matuszewski M. Constructional Features of Ropes in Functional Units of Mining Shaft Hoist. Acta Mechanica et Automatica 2018;12: 66-71, https://doi.org/10.2478/ama-2018-0011.
19. Marandi L, Sen I. Effect of Saline Atmosphere on the Mechanical Properties of Commercial Steel Wire. Metallurgical and Materials Transactions A Physical Metallurgy and Materials Science 2018; 50: 132-141, https://doi.org/10.1007/s11661-018-4956-x.
20. Młynarski S, Pilch R, Smolnik M, Szybka J, Wiązania G. A model of an adaptive strategy of preventive maintenance of complex technical objects. Eksploatacja i Niezawodnosc - Maintenance and Reliability 2020; 22 (1): 35-41, https://doi.org/10.17531/ein.2020.1.5.
21. Pal U, Mukhopadhyay G, Sharma A, Bhattacharya S. Failure analysis of wire rope of ladle crane in steel making shop. International Journal of Fatigue 2018; 116: 149-155, https://doi.org/10.1016/j.ijfatigue.2018.06.019.
22. Pawłowski B, Krawczyk J, Bała P, Cios G, Tokarski T. The analysis of the water-expanded rock bolts ruptures during pressure test. Archives of Mining Sciences 2017; 62: 423-430, https://doi.org/10.1515/amsc-2017-0032.

23. Peng Y X, Chang X D, Sun S S, Zhu Z C, Gong X S, Zou S Y, XU W X, Mi Z T. The friction and wear properties of steel wire rope sliding against itself under impact load. Wear 2018; 400-401: 194-206, https://doi.org/10.1016/j.wear.2018.01.010.

24. Peterka P, Krešák J, Kropuch S, Fedorko G, Molnar V, Vojtko M. Failure analysis of hoisting steel wire rope. Engineering Failure Analysis 2014; 45: 96-105, https://doi.org/10.1016/j.engfailanal.2014.06.005.

25. Peterka P, Krešák J, Šimoňák J, Bindzár P, Kečkešová I. Tractive work of the aerial cableway towing haul rope. Measurement 2017; 100: 322-328, https://doi.org/10.1016/j.measurement.2017.01.006.

26. Piskoty G, Affolter C, Sauder M, Nambiar M, Weisse B. Failure analysis of a ropeway accident focussing on the wire rope's fracture load under lateral pressure. Engineering Failure Analysis 2017; 82: 648-656, https://doi.org/10.1016/j.engfailanal.2017.05.003.

27. Singh R P, Mallick M, Verma M K. Studies on failure behaviour of wire rope used in underground coal mines. Engineering Failure Analysis 2016; 70: 290-304, https://doi.org/10.1016/j.engfailanal.2016.09.002.

28. Vukelic G, Vizentin G. Damage-Induced Stresses and Remaining Service Life Predictions of Wire Ropes. Applied Sciences 2017; 7: 107, https://doi.org/10.3390/app7010107.

29. Wang D, Wang D. Dynamic contact characteristics between hoisting rope and friction lining in the deep coal mine. Engineering Failure Analysis 2016; 64: 44-57, https://doi.org/10.1016/j.engfailanal.2016.03.006.

30. Wang S, Zhang D, Hu N, Zhang J. Effect of stress ratio and loading frequency on the corrosion fatigue behavior of smooth steel wire in different solutions. Materials (Basel) 2016; 9: 9, https://doi.org/10.3390/met7010009.

31. Wang D, Li X, Wang X, Zhang D, Wang D. Dynamic wear evolution and crack propagation behaviors of steel wires during fretting-fatigue. Tribology International 2016; 101: 348-355, https://doi.org/10.1016/j.triboint.2016.05.003.

32 Zhang J, Zheng P, Tan X. Recognition of broken wire rope based on remanence using EEMD and wavelet methods. Sensors 2018; 18: 1-14, https://doi.org/10.3390/s18041110.

33. Zhang J, Tan X, Zheng P. Non-destructive detection of wire rope discontinuities from residual magnetic field images using the hilbert-huang transform and compressed sensing. Sensors 2017; 17: 1-19, https://doi.org/10.3390/s17030608.

34. Zhang D, Feng C, Chen K, Wang D, Ni X. Effect of broken wire on bending fatigue characteristics of wire ropes. International Journal of Fatigue 2017; 103: 456-465, https://doi.org/10.1016/j.ijfatigue.2017.06.024.

35. Zhang S, Sun S, Si S, Wang P. A decision diagram based reliability evaluation method for multiple phased-mission systems. Eksploatacja i Niezawodnosc - Maintenance and Reliability 2017; 19 (3): 485-492, https://doi.org/10.17531/ein.2017.3.20.

36 Zhao B, Zhao ZB, Hua G, Liu C. A new low-carbon microalloyed steel wire in drilling rope. Materials Science and Technology 2016; 32: 722-727, https://doi.org/10.1080/02670836.2016.1152002.

37. Zhao D, Liu S, Xu Q, Shi F, Sun W, Chai L. Fatigue life prediction of wire rope based on stress field intensity method. Engineering Failure Analysis 2017; 81: 1-9, https://doi.org/10.1016/j.engfailanal.2017.07.019.